Polyhedron 27 (2008) 3351–3358

Contents lists available at ScienceDirect

Polyhedron

journal homepage: www.elsevier.com/locate/poly

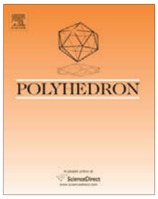

Syntheses and characterizations of nine coordination polymers of transition metals with carboxylate anions and bis(imidazole) ligands

Wen-Li Zhang, Ying-Ying Liu, Jian-Fang Ma *, Hui Jiang, Jin Yang

Key Laboratory of Polyoxometalate Science, Department of Chemistry, Northeast Normal University, Changchun 130024, People's Republic of China

ARTICLE INFO

Article history:
Received 24 May 2008
Accepted 28 July 2008
Available online 25 August 2008

Keywords:
Coordination polymers
Bisimidazole
Carboxylate

ABSTRACT

Nine new compounds, namely [CuL1(biim-6)] · H_2O (**1**), [ZnL1(biim-6)] · H_2O (**2**), [MnL1(biim-6)] · H_2O (**3**), [MnL1(biim-4)] (**4**), [$Co_2(L2)_2(biim\text{-}5)_3$ · $6H_2O$] · $8H_2O$ (**5**), [ZnL3(biim-6)] (**6**), [ZnL3(biim-5)] (**7**), [CdL3(biim-5) · $1.5H_2O$] · $0.5H_2O$ (**8**) and [CdL4(biim-6) · $2H_2O$] (**9**) [where L1 = oxalate anion, L2 = fumarate anion, L3 = phthalate anion, L4 = *p*-phthalate anion, biim-4 = 1,1′-(1,4-butanediyl)bis(imidazole), biim-5 = 1,1′-(1,5-pentanedidyl)bis(imidazole) and biim-6 = 1,1′-(1,6-hexanedidyl)bis(imidazole)] were successfully synthesized. Compounds **1**–**3** are isostructural, and display 2D polymeric structures. Compound **4** shows a threefold interpenetrating diamondoid framework. In compound **5**, the anions act as counterions, and the metal cations are bridged by bis(imidazole) ligands to form 1D polymeric chains. Compounds **6**–**9** show 2D polymeric structures. The magnetic properties for **1**, **3** and **4** and luminescent properties for **2** and **6**–**9** are discussed. Thermogravimetric analyses (TGA) for these compounds are also discussed.

1. Introduction

The design and synthesis of coordination polymers with unusual structures and properties are attracting increasing attention, not only for their intriguing molecular topologies, but also for their potential applications as functional materials [1–3]. The construction of molecular architecture depends on the combination of several factors, like the coordination geometry of metal salt and ligand [4–7]. Thus, understanding how these considerations affect metal coordination and influence crystal packing is at the forefront of controlling coordination supramolecular arrays. Poly-carboxylates are widely used in the assembly of supramolecular architectures because of their diverse coordination modes and bridging abilities [8–12]. Bis(imidazole) ligands bearing alkyl spacers are a good choice of N-donor ligand, and the flexible nature of spacers allows the ligands to bend and rotate when coordinating to metal centers so as to conform to the coordination geometries of metal ions [13–18]. The previous studies show that these ligands exhibit special abilities to formulate the compounds, and the results also indicate that different organic anions play important roles in directing the final structures and topologies [19–22]. In this work, several ternary systems containing transition metals, bis(imidazole) ligands and carboxylate anions are selected to survey the influence factors. We describe the successful syntheses of nine novel compounds: [CuL1(biim-6)] · H_2O (**1**), [ZnL1(biim-6)] · H_2O (**2**), [MnL1(biim-6)] · H_2O (**3**), [MnL1(biim-4)] (**4**), [$Co_2(L2)_2(biim\text{-}5)_3$ · $6H_2O$] · $8H_2O$ (**5**), [ZnL3(biim-6)] (**6**), [ZnL3(biim-5)] (**7**), [CdL3(biim-5) · $1.5H_2O$] · $0.5H_2O$ (**8**) and [CdL4(biim-6) · $2H_2O$] (**9**). The crystal structures of these compounds, along with the systematic investigation of the effect of the anions and the neutral ligands on the ultimate framework, will be represented and discussed (Schemes 1 and 2).

2. Experimental

All reagents and solvents for syntheses were purchased from commercial sources and used as received. Biim-4 [23], biim-5 [24] and biim-6 [23] were synthesized in accordance with the procedure reported. The C, H, and N elemental analysis was conducted on a Perkin–Elmer 240C elemental analyzer. The FT-IR spectra were recorded from KBr pellets in the range 4000–400 cm^{-1} on a Mattson Alpha-Centauri spectrometer. The excitation and emission spectra were measured on a Perkin–Elmer LS55 spectrometer. For the detail syntheses of compounds **1**–**9**, please see Scheme S1 in the Supplementary data.

2.1. Syntheses of the metal complexes

2.1.1. Synthesis of [CuL1(biim-6)] · H_2O (1)

Oxalic acid dihydrate (0.126 g, 1 mmol) was added to the $Cu(OH)_2$ (0.098 g, 1 mmol) suspension in water (10 mL) with stir-

---

* Corresponding author. Tel./fax: +86 431 85098620.
E-mail address: jianfangma@yahoo.com.cn (J.-F. Ma).

0277-5387/$ - see front matter © 2008 Elsevier Ltd. All rights reserved.
doi:10.1016/j.poly.2008.07.026

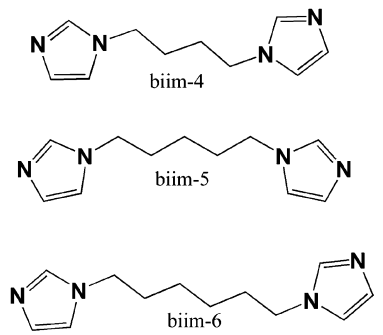

Scheme 1. Structures of bis(imidazole) ligands in this work.

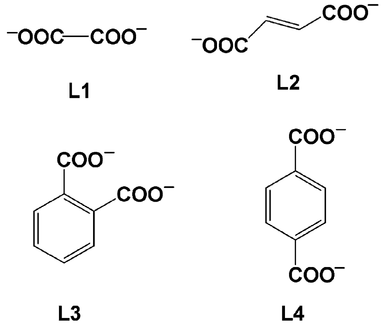

Scheme 2. Structures of the carboxylate anions in this work.

ring. After biim-6 (0.436 g, 2 mmol) in 1 mL ethanol was added, a blue precipitate was obtained. A minimum amount of ammonia (14 M) was added to give a blue solution. Suitable crystals were obtained after standing at room temperature for several days. The crystals were collected in a 75% yield based on Cu^{2+}. Elemental *Anal.* Calc. for $C_{14}H_{20}CuN_4O_5$: C, 43.35; H, 5.20; N, 14.44. Found: C, 43.42; H, 5.27; N, 14.57%. IR (KBr, cm^{-1}): 3741 (w), 3110 (s), 2858 (w), 1613 (s), 1560 (vs), 1516 (vs), 1358 (m), 1229 (m), 1109 (s), 829 (w), 784 (m), 663 (s), 659 (s), 487 (w).

2.1.2. Synthesis of [ZnL1(biim-6)] · H_2O (**2**)

After a mixture of $ZnCO_3$ (0.125 g, 1 mmol), oxalic acid dihydrate (0.126 g, 1 mmol) in water was stirring for 10 min at room temperature, biim-6 (0.436 g, 2 mmol) in 1 mL ethanol was added to the solution with stirring and still precipitate was obtained. A minimum amount of ammonia (14 M) was added to give a colorless solution. Suitable colorless crystals were obtained from the filtrate after standing at room temperature in a 45% yield based on $ZnCO_3$. Elemental *Anal.* Calc. for $C_{14}H_{20}ZnN_4O_5$: C, 43.15; H, 5.26; N, 14.37. Found: C, 43.27; H, 5.31; N, 14.48%. IR (KBr, cm^{-1}): 3741 (s), 3108 (w), 2933 (w), 1652 (vs), 1611 (s), 1454 (s), 1364 (m), 1313 (m), 1229 (w), 828 (s), 790 (s), 492 (m).

2.1.3. Synthesis of [MnL1(biim-6)] · H_2O (**3**)

A mixture of $MnCO_3$ (0.115 g, 1 mmol), oxalic acid dihydrate (0.126 g, 1 mmol) in water (8 mL), and biim-6 (0.436 g, 2 mmol) in ethanol (1 mL) was sealed in a Teflon-lined stainless steel autoclave and heated at 140 °C for 4 days, and then it was cooled to room temperature at 10 °C h^{-1}. Colorless crystals were obtained in a 56% yield based on $MnCO_3$. Elemental *Anal.* Calc. for $C_{14}H_{20}MnN_4O_5$: C, 44.33; H, 5.32; N, 14.77. Found: C, 44.44; H, 5.39; N, 14.70%. IR (KBr, cm^{-1}): 3550 (w), 3413 (m), 3112 (m), 2932 (w), 2858 (w), 1668 (vs), 1615 (vs), 1516 (vs), 1362 (s), 1230 (m), 1227 (m), 1110 (s), 827 (m), 734 (w), 662 (s), 627 (m), 489 (m).

2.1.4. Synthesis of [MnL1(biim-4)] (**4**)

A mixture of $MnCO_3$ (0.115 g, 1 mmol), oxalic acid dihydrate (0.126 g, 1 mmol) in water (8 mL), and biim-4 (0.380 g, 1 mmol) in ethanol (1 mL) was sealed in a Teflon-lined stainless steel autoclave and heated at 140 °C for 4 days prior to being cool to room temperature at 10 °C h^{-1}. Colorless crystals were obtained in a 69% yield based on $MnCO_3$. Elemental *Anal.* Calc. for $C_{12}H_{14}MnN_4O_4$: C, 43.26; H, 4.24; N, 16.81. Found: C, 43.14; H, 4.27; N, 16.75%. IR (KBr, cm^{-1}): 3742 (s), 3116 (w), 2928 (w), 1679 (vs), 1652 (vs), 1618 (m), 1515 (vs), 1389 (m), 1229 (w), 1111 (w), 789 (w), 667 (s), 475 (m).

2.1.5. Synthesis of $[Co_2(L2)_2(biim\text{-}5)_3 \cdot 6H_2O] \cdot 8H_2O$ (**5**)

A mixture of $CoCO_3$ (0.119 g, 1 mmol), fumaric acid (0.116 g, 1 mmol) in water was stirring for 10 min at room temperature. Then biim-5 (0.408 g, 2 mmol) was added to the mixture with stirring for 1 h and pink solution was obtained. Pink crystals were obtained from the filtrate after standing at room temperature for several days in a 75% yield based on $CoCO_3$. Elemental *Anal.* Calc. for $C_{41}H_{80}Co_2N_{12}O_{22}$: C, 40.66; H, 6.66; N, 13.88. Found: C, 40.74; H, 6.70; N, 13.95%. IR (KBr, cm^{-1}): 3670 (w), 3136 (m), 2945 (w), 2858 (w), 1568 (vs), 1455 (m), 1240 (vs), 1108 (vs), 991 (m), 843 (s), 763 (s), 663 (vs).

2.1.6. Synthesis of [ZnL3(biim-6)] (**6**)

A mixture of $ZnCO_3$ (0.125 g, 1 mmol), phthalic anhydride (0.148 g, 1 mmol) in water (8 mL), and biim-6 (0.437 g, 2 mmol) in ethanol (1 mL) was sealed in a Teflon-lined stainless steel autoclave and heated at 180 °C for 4 days, and then it was cooled to room temperature at 10 °C h^{-1}. Colorless crystals were obtained in a 60% yield based on $ZnCO_3$. Elemental *Anal.* Calc. for $C_{20}H_{22}ZnN_4O_4$: C, 53.65; H, 4.95; N, 12.51. Found: C, 53.77; H, 4.97; N, 12.65%. IR (KBr, cm^{-1}): 3123 (w), 3090 (w), 2865 (w), 1619 (vs), 1560 (vs), 1524 (s), 1475 (m), 1377 (vs), 1249 (m), 1144 (m), 950 (m), 768 (s), 655 (vs), 454 (w).

2.1.7. Synthesis of [ZnL3(biim-5)] (**7**)

A mixture of $ZnCO_3$ (0.125 g, 1 mmol), phthalic anhydride (0.148 g, 1 mmol) in water (8 mL), and biim-5 (0.408 g, 2 mmol) in ethanol (1 mL) was sealed in a Teflon-lined stainless steel autoclave and heated at 170 °C for 4 days, and then it was cooled to room temperature at 10 °C h^{-1}. Colorless crystals were obtained in a 66% yield based on $ZnCO_3$. Elemental *Anal.* Calc. for $C_{19}H_{20}ZnN_4O_4$: C, 52.61; H, 4.65; N, 12.92. Found: C, 52.77; H, 4.61; N, 12.81%. IR (KBr, cm^{-1}): 3421 (m), 3111 (m), 2938 (w), 1617 (vs), 1565 (vs), 1516 (s), 1457 (s), 1365 (vs), 1246 (m), 1147 (m), 953 (m), 833 (m), 756 (m), 659 (m), 478 (w).

2.1.8. Synthesis of [CdL3(biim-5) · $1.5H_2O$] · $0.5H_2O$ (**8**)

A mixture of $Cd(OH)_2$ (0.146 g, 1 mmol), phthalic anhydride (0.148 g, 1 mmol) in water (8 mL), and biim-5 (0.408 g, 2 mmol) in ethanol (1 mL) was sealed in a Teflon-lined stainless steel autoclave and heated at 170 °C for 4 days, and then it was cooled to room temperature at 10 °C h^{-1}. Colorless crystals were obtained in a 56% yield based on $Cd(OH)_2$. Elemental *Anal.* Calc. for $C_{19}H_{24}CdN_4O_6$: C, 44.16; H, 4.68; N, 10.84. Found: C, 44.27; H, 4.60; N, 10.95%. IR (KBr, cm^{-1}): 3742 (w), 3118 (w), 2933 (w), 2862 (w), 1646 (m), 1560 (vs), 1516 (s), 1481 (m), 1397 (vs), 1235 (m), 1112 (m), 937 (m), 841 (m), 751 (s), 652 (vs), 438 (s).

2.1.9. Synthesis of [CdL4(biim-6) · $2H_2O$] (**9**)

A mixture of $Cd(OH)_2$ (0.146 g, 1 mmol), *p*-phthalic acid (0.166 g, 1 mmol) in water (8 mL), and biim-6 (0.436 g, 2 mmol) in ethanol (1 mL) was sealed in a Teflon-lined stainless steel autoclave and heated at 180 °C for 4 days, and then it was cooled to room temperature at 10 °C h^{-1}. Colorless crystals were obtained in a 67% yield based on $Cd(OH)_2$. Elemental *Anal.* Calc. for $C_{20}H_{26}CdN_4O_6$: C, 45.25; H, 4.94; N, 10.55. Found: C, 45.17; H, 4.86; N, 10.42%. IR (KBr, cm^{-1}): 3743 (w), 3414 (vs), 2935 (w), 2862 (w), 1643 (s), 1616 (s), 1560 (vs), 1515 (s), 1465 (s), 1383 (vs), 1235 (w), 1116 (m), 745 (m), 651 (m), 452 (m).

2.2. X-ray crystallography

Single-crystal X-ray diffraction data for compounds **1, 2** and **4** were recorded on a Bruker Apex CCD diffractometer with graphite-monochromated Mo Kα radiation ($\lambda = 0.71073$ Å) at 293 K. Crystallographic data for compounds **3** and **5–9** were collected on a Rigaku RAXIS-RAPID single-crystal diffractometer with Mo Kα radiation ($\lambda = 0.71073$ Å) at 293 K. Absorption corrections were applied using multi-scan technique. All the structures were solved by Direct Method of SHELXS-97 [25] and refined by full-matrix least-squares techniques using the SHELXL-97 program [26] within WINGX [27]. Non-hydrogen atoms were refined with anisotropic temperature parameters. The hydrogen atoms attached to carbons were generated geometrically; the aqua hydrogen atoms were located from difference Fourier maps and refined with isotropic displacement parameters. Analytical expressions of neutral-atom scattering factors were employed, and anomalous dispersion corrections were incorporated [28]. The disordered C atoms in compounds **4** and **5** and disordered O atoms in compound **8** were refined using C or O atoms split over two sites, with a total occupancy of 1. The water H atoms in compounds **1**–**3** and **8** could not be positioned reliably and were omitted from the final model. The bond distance restraints were used in the refinement for the water molecules in compound **5**.

Detailed crystallographic data and structure refinement parameters for **1**–**9** are summarized in Table 1. Selected bond distances and angles for compounds **1**–**9** are listed in Table S1 (see the Supplementary data).

3. Results and discussion

3.1. Descriptions of crystal structures

3.1.1. Structure of [CuL1(biim-6)] · H_2O (**1**)

Compounds **1**–**3** are isostructural and crystallize in the monoclinic *C*2/*c* space groups; therefore the structure descriptions of compounds **2** and **3** will be neglected.

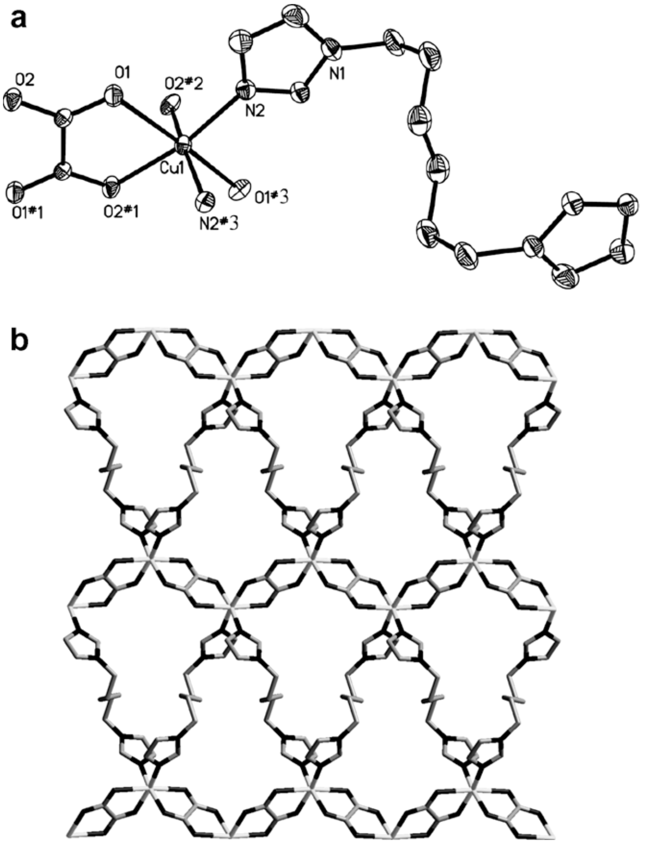

Fig. 1. (a) Coordination environment of the copper cation in **1**. (b) View of a single layer of **1**.

As shown in Fig. 1a, each Cu(II) atom lies on an inversion center and six-coordinated by four O atoms from two oxalate anions (Cu–O 2.006(1)–2.321(1) Å) and two N atoms from biim-6 ligands (Cu–N 2.011(2) Å). Due to the Jahn–Teller effect, the Cu–O distance of axial site is much longer than those in the equatorial plane. Each oxalate anion coordinates to two Cu atoms to form a 1D chain with a Cu···Cu distance of 5.58 Å. The neutral ligand biim-6 connects two Cu atoms and a 2D network is obtained (Fig. 1b).

3.1.2. Structure of [MnL1(biim-4)] (**4**)

As illustrated in Fig. 2a, each central Mn(II) atom in **4** is coordinated by four O atoms (Mn–O 2.199(3)–2.211(3) Å) of two oxalate anions and two N atoms (Mn–N 2.198(4)–2.231(4) Å) from biim-4

Table 1
Crystal data and structure refinements for compounds **1**–**9**

	1	**2**	**3**	**4**	**5**	**6**	**7**	**8**	**9**
Formula	$C_{14}H_{20}CuN_4O_5$	$C_{14}H_{20}N_4O_5Zn$	$C_{14}H_{20}MnN_4O_5$	$C_{12}H_{14}MnN_4O_4$	$C_{41}H_{80}Co_2N_{12}O_{22}$	$C_{20}H_{22}ZnN_4O_4$	$C_{19}H_{20}ZnN_4O_4$	$C_{19}H_{24}CdN_4O_6$	$C_{20}H_{26}CdN_4O_6$
Molecular weight	387.88	389.71	379.28	333.21	1211.03	447.79	433.76	516.82	530.85
Crystal system	monoclinic	monoclinic	monoclinic	triclinic	triclinic	triclinic	orthorhombic	monoclinic	triclinic
Space group	*C*2/*c*	*C*2/*c*	*C*2/*c*	$P\bar{1}$	$P\bar{1}$	$P\bar{1}$	*Pbca*	*C*2/*c*	$P\bar{1}$
a (Å)	12.721(9)	12.758(7)	12.640(3)	8.056(2)	9.021(3)	9.677(4)	10.340(2)	16.591(7)	5.669(2)
b (Å)	13.578(8)	13.876(8)	14.330(3)	9.889(3)	13.004(5)	9.968(5)	13.539(3)	16.472(4)	8.868(6)
c (Å)	9.624(9)	9.437(7)	9.680(2)	9.989(2)	25.752(7)	11.716(6)	27.813(7)	14.641(6)	10.497(8)
α (°)	90	90.	90	103.585(4)	82.51(1)	78.69(2)	90	90	76.781(3)
β (°)	99.761(1)	99.557(2)	98.400(9)	97.253(6)	86.76(1)	74.02(3)	90	92.564(2)	86.480(4)
γ (°)	90	90	90	107.040(4)	71.12(1)	68.61(4)	90	90	84.391(3)
V ($Å^3$)	1638(2)	1648(2)	1734.5(7)	723.1(3)	2834(2)	1005.8(9)	3894(1)	3997(3)	510.9(6)
Z	4	4	4	2	2	2	8	8	1
Goodness-of-fit	1.127	1.036	1.176	1.031	1.061	1.050	1.046	1.006	1.085
$R_1[I > 2\sigma(I)]$	0.0309	0.0450	0.1016	0.0630	0.0461	0.0330	0.0345	0.0568	0.0399
wR_2 [all data]	0.0895	0.1323	0.1994	0.1709	0.1276	0.0764	0.0811	0.1291	0.0780

$R_1 = \sum||F_o| - |F_c||/\sum|F_o|$, $wR_2 = |\sum w(|F_o|^2 - |F_c|^2)|/\sum|w(F_o^2)^2|^{1/2}$.

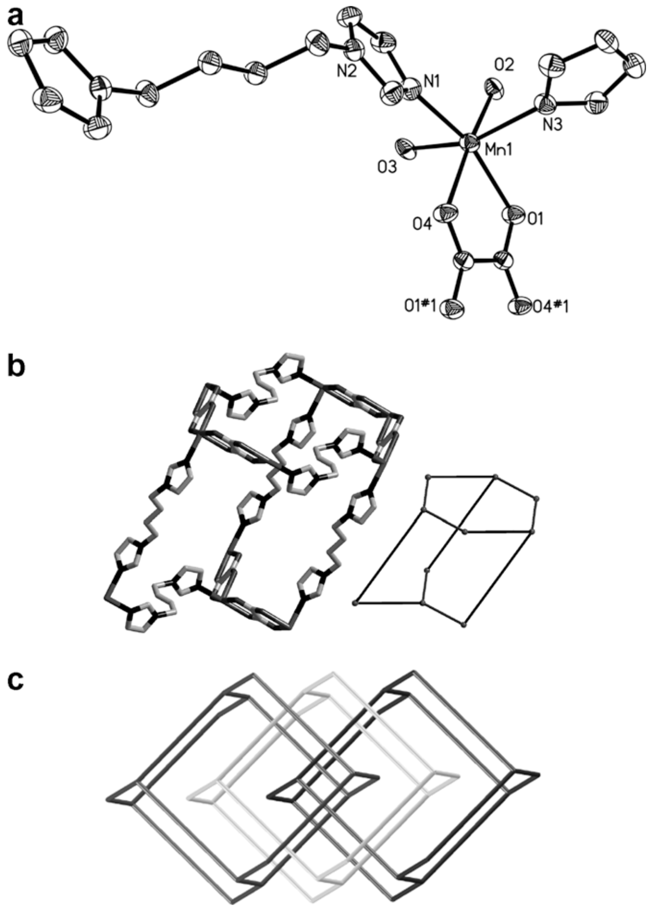

Fig. 2. (a) Coordination environment of the manganese cation in **4**. (b) Single adamantanoid cage. (c) Three interpenetrating diamondoid cages.

ligands to furnish a disordered octahedron geometry. Two crystallographically biim-4 ligands adopt "*S*" shaped and "zigzag" shaped conformations, respectively. The topology of the whole structure can be described as a typically diamondoid framework (Fig. 2b). As can be seen, the diamondoid cage are elongated significantly in one direction, and exhibit maximum dimensions (corresponding to the longest intracage Mn$\cdots$Mn distances) of 21.37 Å × 20.18 Å × 18.90 Å. Because of the spacious nature of the single network, it allows two identical diamondoid networks to interpenetrate it in a normal mode giving rise to a threefold interpenetrating structure (Fig. 2c). According to topology classification, compound **4** belongs to Class Ia (all the independent nets are related by a single vector and the whole interpenetrating arrays are generated by translating a single net 2 times) [29], with the translating vector of [1 0 0] (8.06 Å).

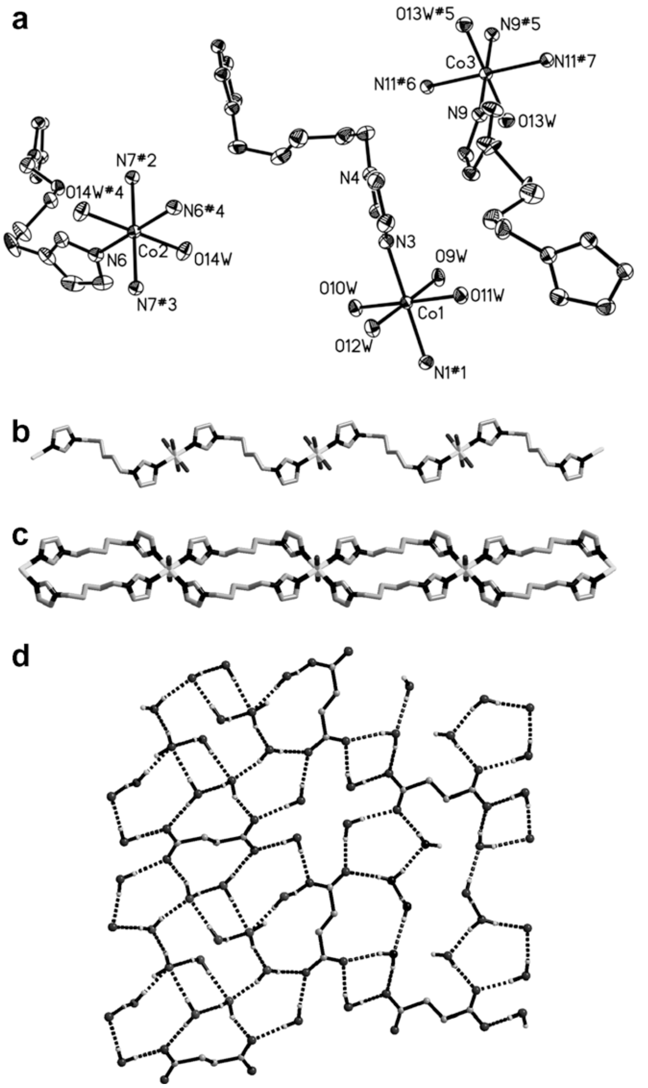

Fig. 3. (a) Coordination environment of the cobalt cations in **5**. (b) View of single chain composed of Co1 and biim-5 ligands. (c) View of double-stranded chain composed of Co2, Co3 and biim-5 ligands. (d) The hydrogen-bonded layer of L2 and water molecules.

3.1.3. Structure of $[Co_2(L2)_2(biim\text{-}5)_3 \cdot 6H_2O] \cdot 8H_2O$ (**5**)

As shown in Fig. 3a, there are three kinds of crystallographically unique Co centers in the structure of **5**. Co1 is coordinated by two N atoms (Co–N 2.111(2)–2.112(2) Å) from two neutral ligands and four water molecules (Co–O 2.095(2)–2.153(2) Å), showing a slightly disordered octahedral geometry. Co2 lies at an inversion center and is six-coordinated by four N atoms (Co–N 2.128(2)–2.137(2) Å) from biim-5 ligands and two water molecules (Co–O 2.154(2) Å). Co3 has the same coordination environment to that of Co2. The fumariate anions act as counterions. There exist two kinds of chains. For Co1, each biim-5 ligand connects two Co1 atoms to a 1D polymeric chain (Fig. 3b). For Co2 and Co3, the Co(II) atoms are joined by biim-5 ligands to form a double-stranded chain (Fig. 3c). These two kinds of chains are connected by hydrogen bonds to construct a 3D supramolecular structure (Fig. S1a). As shown in Fig. 3d, the hydrogen bonds lead the water molecules and L2 anions to a 2D supramolecular network. In addition, a notable feature of **6** is the presence of two types of water clusters, namely $(H_2O)_{12}$ and $(H_2O)_8$. Within the $(H_2O)_{12}$ cluster, four water molecules (O8W, O8W$^{\#13}$, O13W$^{\#5}$ and O13W$^{\#12}$, symmetry code: $^{\#5}-x+1, -y+1, -z$; $^{\#12}1+x, y, z$; $^{\#13}2-x, 1-y, -z$) act as hydrogen bonds donors and others act as both donors and acceptors (Fig. S1b). In this water cluster, O1W$^{\#2}$, O2W, O6W$^{\#5}$, O13W$^{\#5}$ and O1W$^{\#3}$, O2W$^{\#13}$, O6W$^{\#12}$, O13W$^{\#12}$ (symmetry code: $^{\#2}-x, -y+2, -z$; $^{\#3}1+x, -1+y, z$) form two types 4-membered $(H_2O)_4$ rings, respectively and these rings are connected by O7W$^{\#2}$ and O7W$^{\#3}$ to form a much lager $(H_2O)_{10}$ ring. The $(H_2O)_{10}$ ring are joined by O8W and O8W$^{\#13}$ to form a $(H_2O)_{12}$ cluster. Moreover, the oxygen atoms O2, O3, O19 and O9 from L2 anions are involved in hydrogen bonds with water molecules, which helped to stabilize the $(H_2O)_{12}$ cluster. In $(H_2O)_{12}$ cluster, the average hydrogen bond is 2.78 Å, while these distances in regular ice, liquid water, and water vapor are 2.74, 2.85, and 2.98 Å, respectively [30]. In $(H_2O)_8$ cluster, four crystallographically unique lattice water molecules (O3W$^{\#8}$, O4W and O5W$^{\#9}$ act as both hydrogen-bond donors

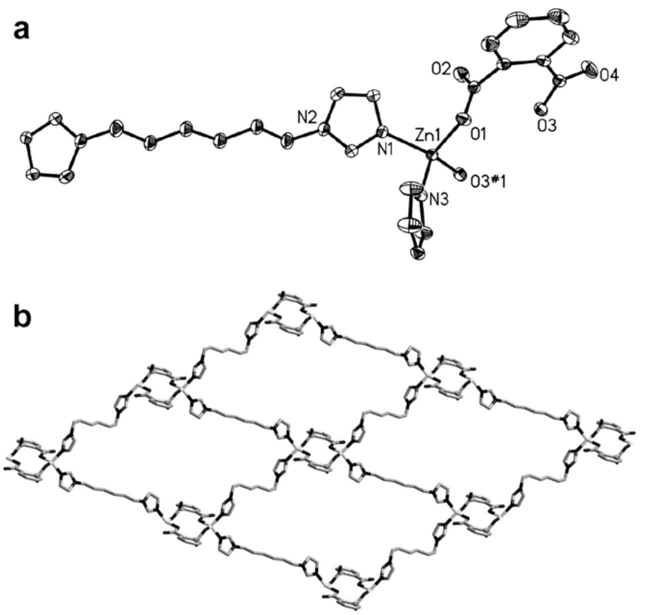

Fig. 4. (a) Coordination environment of the zinc cation in **6**. (b) View of a single layer.

and acceptors, while O14W$^{\#4}$ only acts as a hydrogen-bond donor) and their symmetry-related molecules link to each other to form a $(H_2O)_8$ cluster through hydrogen bonds (Fig. S1c). Furthermore, the oxygen atoms O1, O6$^{\#14}$, O21 and O22$^{\#8}$ from L2 anions (symmetry code: $^{\#14}2-x$, $1-y$, $1-z$) are involved in hydrogen bonds with water molecules to stabilize the $(H_2O)_8$ cluster.

*3.1.4. Structure of [ZnL3(biim-6)] (**6**)*

In compound **6**, L3 was introduced to replace L1 ligand of compound **2**. As illustrated in Fig. 4a, each Zn(II) atom is four-coordinated by two O atoms (Zn–O 1.951(2)–1.957(2) Å) from two L3 anions and two N atoms (Zn–N 2.003(2)–2.035(2) Å) from biim-6 ligands to furnish a distorted tetrahedron geometry. The phthalate anions adopt bis(monodentate) coordination mode to connect two central Zn(II) atoms. Every two L3 anions coordinate with the same two Zn(II) atoms and form a dimer. Biim-6 ligands display two kinds of conformations, which link the dimers to a 2D layer network (Fig. 4b).

*3.1.5. Structure of [ZnL3(biim-5)] (**7**)*

As shown in Fig. 5a, every Zn(II) atom in **7** is four-coordinated by two O atoms from two L3 anions and two N atoms from two biim-5 ligands. The L3 anion adopts bis(monodentate) coordination mode and connects two Zn(II) atoms. As bridged ligand, each biim-5 connects two Zn(II) atoms to form a dimer (Fig. 5b). These dimers are connected by L3 anions to a 2D network with (6,3) topology (Fig. 5c).

*3.1.6. Structure of [CdL3(biim-5) · 1.5H$_2$O] · 0.5H$_2$O (**8**)*

In compound **8**, cadmium ion was introduced to replace zinc ion in compound **7**. As illustrated in Fig. 6a, each Cd(II) atom is eight-coordinated by four O atoms (Cd–O 2.359(5)–2.626(7) Å) [31,32] from two L3 anions, two N atoms (Cd–N 2.264(5)–2.278(5) Å) from two biim-5 ligands and two water molecules (Cd–O 2.487(6)–2.56(2) Å). Two L3 anions connect to the same two Cd(II) atoms in the chelating modes to form a dimer (Fig. 6b). These dimers are joined by biim-5 ligands to a 2D layer network (Fig. 6b).

*3.1.7. Structure of [CdL4(biim-6) · 2H$_2$O] (**9**)*

As illustrated in Fig. 7a, each Cd(II) atom in **9** lies on an inversion center and is six-coordinated by two O atoms from two L4 anions, two N atoms from two biim-6 ligands and two water molecules. Each L4 adopts bis(monodentate) coordination mode and connects with two Cd(II) atoms to a 1D chain. These chains are joined by biim-6 ligands to propagate a 2D layer network (Fig. 7b). In addition, hydrogen bonds between L4 and water molecules exist in **9**. These hydrogen bonds link L4 anions and water molecules resulting a 1D infinite chain. These chains stabilize the structure and connect the adjacent layers to form a 3D supramolecular structure (Fig. 7c).

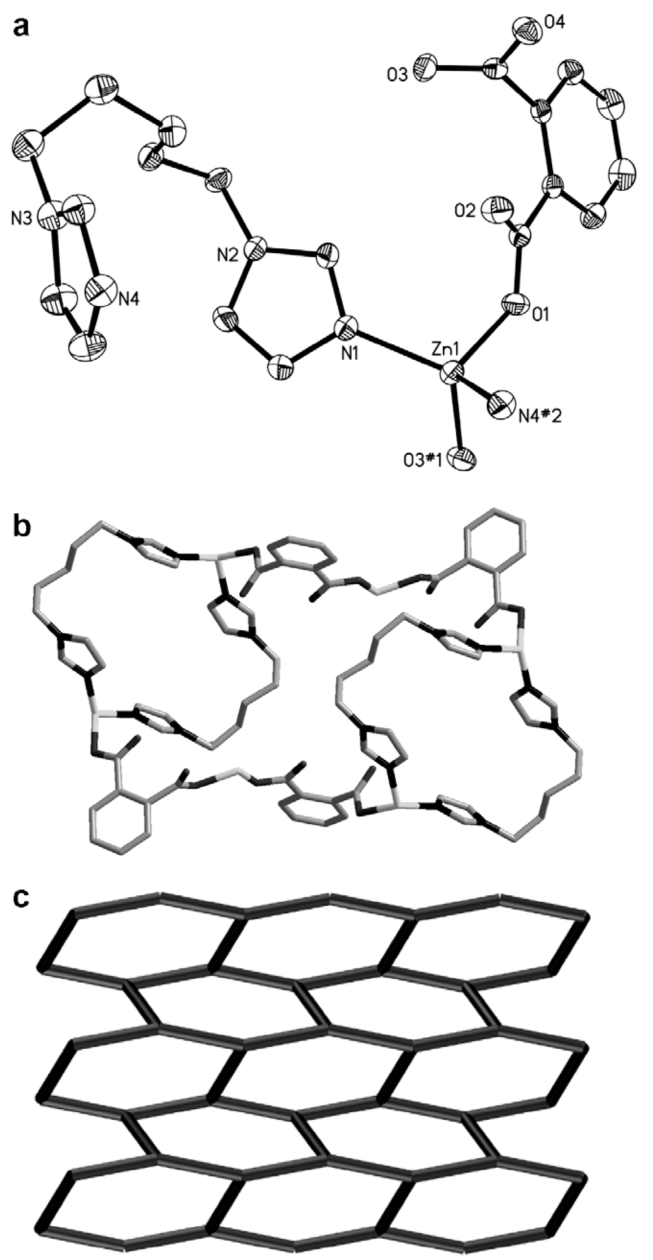

Fig. 5. (a) Coordination environment of the zinc cation in **7**. (b) View of the large ring of (6, 3) network. (c) View of a layer of (6, 3) topology.

3.2. Discussion

3.2.1. Effect of carboxylate anions

As expected, carboxylate anion plays an important role in determining the final structures. All of the L1 anions in **1**-**4** adopt bis(chelating) coordination modes, and M(II) centers are bridged

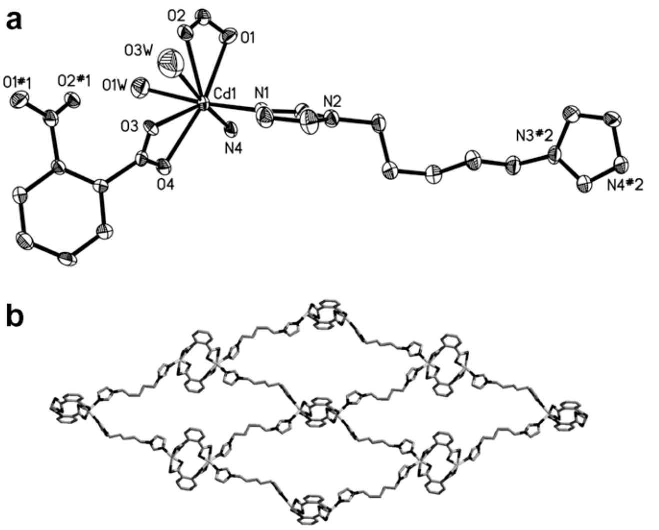

Fig. 6. (a) Coordination environment of the cadmium cation in **8**. (b) View of a single layer of compound **8**.

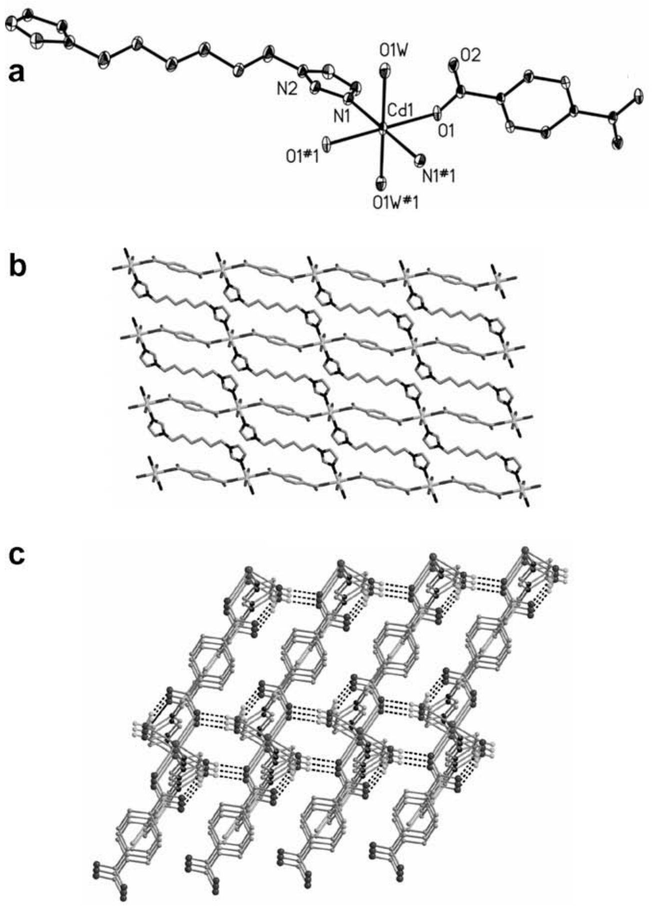

Fig. 7. (a) Coordination environment of the cadmium cation in **9**. (b) View of a single layer. (c) View of the 3D supramolecular structure formed by hydrogen bonds.

by L1 anions to form 1D chain skeletons. L2 anions in **5** act as counterions. Although the L2 anions in **5** are not coordinated with Co(II) ions, they joined by hydrogen bonds with water molecules, which also modulate the whole structure of **5**. L3 anions in **6** and **7** adopt bis(monodentate) coordination modes; and L3 anion in **8** adopts bis(chelating) coordination mode. The M(II) centers in **6** and **8** are linked by L3 anions to dimers, respectively, and the M(II) centers in **7** are linked by L3 anions to a chain. L4 anion in **9** adopts bis(monodentate) mode, and the L4 anions link M(II) center to form a chain.

3.2.2. Effect of bis(imidazole) ligands

In the structures of biim-6, biim-5 and biim-4, the imidazole groups are bridged by different spacers: 1,6-hexyl, 1,5-pentyl and 1,4-butyl. By comparing of the structures of compounds **1**–**9**, it was found that the flexibilities of the bis(imidazole) methylene groups have a great influence to the frameworks, because adjustments in the framework occur to accommodate the bend of the molecules. In compounds **1**–**3**, **6** and **9**, the neutral ligands are biim-6. The methylene groups of **1**–**3** display "*S*" conformations, with the distance between neighboring M(II) centers linked by biim-6 ligands being 11.77–12.34 Å. The methylene groups of **6** and **9** display zigzag conformations, with the distance between neighboring M(II) centers linked by biim-6 ligands being 14.19–16.49 Å. In compounds **5**, **7** and **8**, the neutral ligands are biim-5, and the methylene groups display "*S*" and "3" formed conformations, the distance between neighboring M(II) centers linked by biim-5 ligands are 8.39–15.12 Å. In compounds **4**, the neutral ligand is biim-4, and the methylene groups display "*S*" and zigzag conformations, with the distance between neighboring Mn(II) centers linked by the biim-4 ligands being 13.74 and 14.06 Å.

Comparing compounds **6** with **7**, it can be seen that the neutral ligands biim-6 of **6** display two kinds of conformations. The [Zn(L3)$_2$Zn] dimers are linked by biim-6 to a 2D network (Fig. 4b). In **7**, biim-5 adopt only one kind of conformation to connect the central Zn(II) atoms to [Zn(biim-5)$_2$Zn] dimers (Fig. 5b). By comparing **3** with **4**, the changes are more noticeable. Compound **3** has a 2D layer network, while compound **4** displays a 3D network with diamondoid topology.

3.3. Thermal analysis

In order to characterize the compounds more fully in terms of thermal stability, some of their thermal behaviors were studied by TGA (Fig. S2). The experiments were performed on samples consisting of numerous single crystals of **3**, **5** and **8**–**9** under N_2 atmosphere with a heating rate of 10 °C/min.

For compound **3**, the weight loss corresponding to the release of water molecules are observed from room temperature to 135 °C (obsd 3.9%, calcd 4.75%). The anhydrous compound begins to decompose at 253 °C. For compound **5**, the weight loss corresponding to the release of water molecules are observed from room temperature to 105 °C (obsd 19.1%, calcd 20.83%). The anhydrous compound begins to decompose at 253 °C. For compound **8**, the weight loss corresponding to the release of water molecules are observed from room temperature to 175 °C (obsd 4.7%, calcd 3.57%). The anhydrous compound begins to decompose at 240 °C. For compound **9**, the weight loss corresponding to the release of water molecules are observed from 120 to 236 °C (a weight loss of 5.1% is smaller than the calculated value 6.78% probably resulting from a slow losing of the guest molecules in the air at room temperature). The anhydrous compound begins to decompose at 305 °C.

3.4. Luminescent properties

The luminescence spectra of neutral ligands biim-5 and biim-6 were examined in an ethanol solution, because the solid samples cannot be isolated at room temperature (Table 2, Fig. S3). The solid state luminescence spectra of free carboxylate ligands, compounds

Table 2
The wavelengths of the emission maximums and excitation (nm)

Compound	2	6	7	8	9
λ_{em}	403	427	406	441	429
λ_{ex}	348	315	346	366	352
Ligand	Biim-5	Biim-6	Phthalic anhydride		H_2L4
λ_{em}	400	363, 379	389		390
λ_{ex}	342	343	352		347

2 and **6**–**9** were examined at room temperature (Table 2, Figs. S4 and S5).

Biim-5 shows an emission at 400 nm; and biim-6 shows a maximum at 379 nm and a shoulder at 363 nm. The peaks of the ligands biim-5 and biim-6 are probably due to $\pi^* \to \pi$ transitions [33].

The emissions of free ligands of phthalic anhydride (389, $\lambda_{ex} = 352$ nm) and H_2L4 (390 nm, $\lambda_{ex} = 347$ nm) [34] can also exhibit fluorescence at room temperature. The emission bands of the dicarboxylate ligands can be assigned to the $\pi^* \to n$ transitions [35]. The Zn(II) compounds (**2**, **6** and **7**) exhibit emissions at about 403 nm for **2**, at 427 nm for **6**, and at 406 nm for **7**. The emission peaks for these compounds may be attributed to the ligand-to-metal charge-transfer (LMCT) transitions [36,37]. The luminescent spectra of Cd(II) compounds **8** (441 nm) and **9** (429 nm) may also be assigned as LMCT [37].

3.5. Magnetic properties

The temperature-dependent magnetic susceptibility data of compounds **1**, **3** and **4** have been measured from polycrystalline samples at an applied magnetic field of 1000 Oe in the temperature range of 2–300 K (Fig. 8). Although compounds **1** and **3** are two-dimensional, and **4** is three-dimensional, from a magnetic point of view, the systems can be considered as one-dimensional owing to the long M···M distances (11.77 Å for **1**, 12.34 Å for **3** and 12.46 Å for **4**) along the bis(imidazole) ligands, for which we can assume a negligible magnetic exchange through the biim-6 and biim-4 ligands [38].

For **1**, the $\chi_m T$ value at 300 K is 0.451 cm^3 mol^{-1} K (1.900 μ_B), which is as expected (1.732 μ_B, considering $g = 2.00$) for a magnetically isolated spin doublet. Upon cooling, $\chi_m T$ gradually increase, reaching a value of 0.551 cm^3 mol^{-1} K at 2 K. This feature is indicative of the occurrence of an overall weak ferromagnetic coupling between the Cu(II) ions [39–43]. The magnetic susceptibility in the range of 300–100 K obeys the Curie–Weiss law with the Curie constant, $C = 0.451$ cm^3 mol^{-1} K, and the Weiss constant, $\Theta = 0.329$ K.

For **3**, the $\chi_m T$ value at 300 K is 5.077 cm^3 mol^{-1} K (6.372 μ_B), which is slightly higher than the spin-only value (5.916 μ_B, considering g = 2.00) expected for a high-spin d^5 Mn(II) ion. Upon cooling, the values of $\chi_m T$ keep smoothly decreasing in 300–34 K range, and then exhibit a maximum value of 2.899 cm^3 mol^{-1} K at 32 K before goes down quickly to a minimum value of 0.186 cm^3 mol^{-1} K at 2 K. This behavior is indicative of antiferromagnetic coupling between the Mn(II) centers through the oxalate-bridging ligands. The inflexion at 32 K may be due to a small canting of the sub-lattice or a small amount of impurity [34]. The magnetic susceptibility above 34 K can be well fit to Curie–Weiss law with $C = 5.66$ cm^3 mol^{-1} K, $\Theta = -35.62$ K. The negative Θ value further confirms the presence of antiferromagnetic interaction in **3**.

The magnetic behavior of compounds **3** and **4** is quite similar. For **4**, the $\chi_m T$ value at 300 K is 4.841 cm^3 mol^{-1} K (6.223 μ_B). Upon cooling, the values of $\chi_m T$ keep smoothly decreasing in 300–34 K range, and then go down quickly to a minimum value of 0.183 cm^3 mol^{-1} K at 2 K, indicating an overall antiferromagnetic coupling in compound **4**. There also exists an inflexion at 32 K [44]. The magnetic susceptibility above 34 K can be well fit to Curie–Weiss law with $C = 5.38$ cm^3 mol^{-1} K, $\Theta = -35.06$ K.

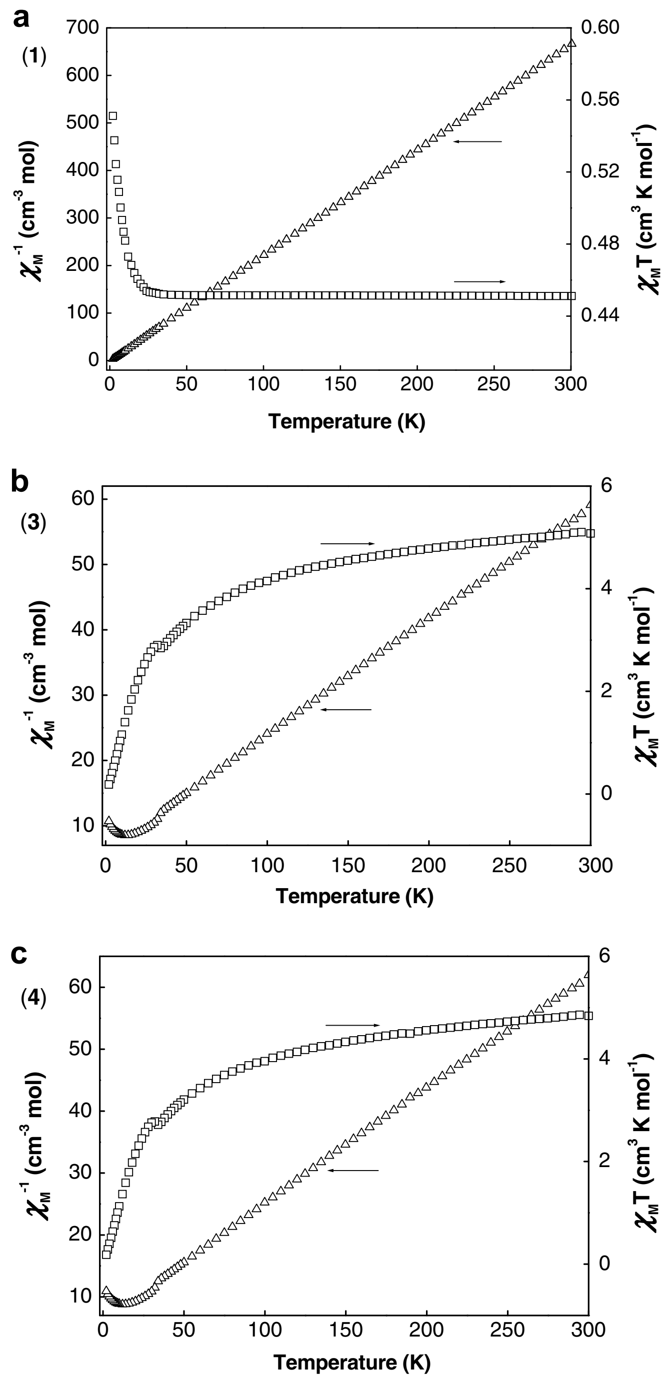

Fig. 8. Plots of the temperature dependence of $\chi_m T$ (squares) and χ_m^{-1} (triangles) for compounds **1**, **3** and **4**.

Acknowledgments

We thank the Program for New Century Excellent Talents in Chinese University (NCET-05-0320), Program for Changjiang Scholars and Innovative Research Teams in Chinese University and the Analysis and Testing Foundation of Northeast Normal University for support.

Appendix A. Supplementary data

CCDC 671105–671113 contain the supplementary crystallographic data for **1**–**9**. These data can be obtained free of charge via http://www.ccdc.cam.ac.uk/conts/retrieving.html, or from the Cambridge Crystallographic Data Centre, 12 Union Road, Cambridge CB2 1EZ, UK; fax: (+44) 1223-336-033; or e-mail: deposit@ccdc.cam.ac.uk. Supplementary data associated with this article can be found, in the online version, at doi:10.1016/j.poly.2008.07.026.

References

[1] S. Kitagawa, R. Kitaura, S.I. Noro, Angew. Chem., Int. Ed. 43 (2004) 2334.
[2] O.R. Evans, W. Lin, Acc. Chem. Res. 35 (2002) 511.
[3] X.H. Bu, M.L. Tong, H.C. Chang, S. Kitagawa, S.R. Batten, Angew. Chem., Int. Ed. 43 (2004) 192.
[4] M. Munakata, L.P. Wu, T. Kuroda-Sowa, M. Maekawa, K. Moriwaki, S. Kitagawa, Inorg. Chem. 36 (1997) 5416.
[5] Y. Suenaga, S.G. Yan, L.P. Wu, I. Ion, T. Kuroda-Sowa, M. Maekawa, M. Munakata, J. Chem. Soc., Dalton Trans. 23 (1998) 1121.
[6] K.A. Hirsch, S.R. Wilson, J.S. Moore, Inorg. Chem. 36 (1997) 2960.
[7] L. Carlucci, G. Ciani, P. Macchi, D.M. Proserpio, A. Sironi, Chem. Commun. (1997) 631.
[8] B.-H. Ye, M.-L. Tong, X.-M. Chen, Coord. Chem. Rev. 249 (2005) 545.
[9] J. Yang, Q. Yue, H.M. Yuan, J.S. Chen, S.N. Wang, Inorg. Chem. 45 (2006) 2857.
[10] C.N.R. Rao, S. Natarajan, R. Vaidhyanathan, Angew. Chem., Int. Ed. 43 (2004) 1466.
[11] G. Férey, C. MellotDraznieks, C. Serre, F. Millange, Acc. Chem. Res. 38 (2005) 217.
[12] X.-L. Wang, C. Qin, E.-B. Wang, Z.-M. Su, Chem. Eur. J. 12 (2006) 2680.
[13] B.F. Hoskins, R. Robson, D.A. Slizys, J. Am. Chem. Soc. 119 (1997) 2952.
[14] E.-Q. Gao, Y.-X. Xu, C.-H. Yan, CrystEngComm. 6 (2004) 298.
[15] J. Fan, C. Slebodnick, R. Angel, B.E. Hanson, Inorg. Chem. 44 (2005) 552.
[16] L. Zhang, X.-Q. Lü, C.-L. Chen, H.-Y. Tan, H.-X. Zhang, B.-S. Kang, Cryst. Growth Des. 5 (2005) 283.
[17] X. Li, R. Cao, W. Bi, Y. Wang, Y. Wang, X. Li, Z. Guo, Cryst. Growth Des. 5 (2005) 1651.
[18] G.-H. Cui, J.-R. Li, J.-L. Tian, X.-H. Bu, S.R. Batten, Cryst. Growth Des. 5 (2005) 1775.
[19] J.-F. Ma, J. Yang, G.-L. Zheng, L. Li, J.-F. Liu, Inorg. Chem. 42 (2003) 7531.
[20] J.-F. Ma, J. Yang, G.-L. Zheng, L. Li, Y.-M. Zhang, F.-F. Li, J.-F. Liu, Polyhedron. 23 (2004) 553.
[21] J. Yang, J.-F. Ma, Y.-Y. Liu, J.-C. Ma, H.-Q. Jia, N.-H. Hu, Eur. J. Inorg. Chem. (2006) 1208.
[22] J. Yang, J.-F. Ma, Y.-Y. Liu, S.-L. Li, G.-L. Zheng, Eur. J. Inorg. Chem. (2005) 2174.
[23] Y.-H. So, Macromolecules 25 (1992) 516.
[24] Y. Wang, X.-F. Wang, T.-A. Okanura, B. Xu, W.-Y. Sun, N. Ueyama, Chinese J. Inorg. Chem. 22 (2006) 1487.
[25] G.M. Sheldrick, SHELXS-97 Programs for X-ray Crystal Structure Solution, University of Göttingen, Göttingen, Germany, 1997.
[26] G.M. Sheldrick, SHELXL-97, Programs for X-ray Crystal Structure Refinement, University of Göttingen, Göttingen, Germany, 1997.
[27] L.J. Farrugia, WINGX, A Windows Program For Crystal Structure Analysis, University of Glasgow, Glasgow, UK, 1988.
[28] T. Comer, International Tables for X-ray Crystallography, vol. C, Kluwer Academic Publisher, Dordercht, The Netherlands, 1992.
[29] V.A. Blatov, L. Carlucci, G. Ciani, D.M. Proserpio, CrystEngComm. 6 (2004) 377.
[30] R. Ludwig, Angew. Chem., Int., Ed. 40 (2001) 1808.
[31] J. Zhang, Z.-J. Li, Y. Kang, J.-K. Cheng, Y.-G. Yao, Inorg. Chem. 43 (2004) 8085.
[32] W. Clegg, J.T. Cressey, A. Mcamley, B.P. Straughan, Acta Crystallogr., Sect. C 51 (1995) 234.
[33] Z. Guo, R. Cao, X. Li, D. Yuan, W. Bi, X. Zhu, Y. Li, Eur. J. Inorg. Chem. (2007) 742.
[34] W. Chen, J.-Y. Wang, C. Chen, H.-M. Yuan, J.-S. Chen, S.-N. Wang, Inorg. Chem. 42 (2003) 944.
[35] Y.-S. Song, B. Yan, Z.-X. Chen, J. Solid State Chem. 179 (2006) 4037.
[36] J. Tao, M.L. Tong, J.X. Shi, X.M. Chen, S.W. Ng, Chem. Commun. (2000) 2043.
[37] M. Li, J. Xiang, L. Yuan, S. Wu, S. Chen, J. Sun, Cryst. Growth Des. 6 (2006) 2036.
[38] O. Kahn, Molecular Magnetism, VCH, Weinheim, Germany, 1993. references therein.
[39] P. Day, Science 261 (1993) 431.
[40] S. Decurtins, H.W. Schmalle, P. Schneuwly, R. Schneuwly, L.M. Zheng, J. Ensling, A. Hauser, Inorg. Chem. 34 (1995) 5501.
[41] E. Coronado, J.R. Galán-Mascarós, C. Martí-Gastaldo, Inorg. Chem. 45 (2006) 1882.
[42] E. Coronado, P. Day, Chem. Rev. 104 (2004) 5419.
[43] U. García-Couceiro, O. Castillo, A. Luque, J.P. García-Terán, G. Beobide, P. Román, Cryst. Growth Des. 6 (2006) 1839.
[44] M.B. Salah, S. Vilminot, T. Mhiri, M. Kurmoo, Eur. J. Inorg. Chem. (2004) 2272.